Major Category: Biological Sciences
Minor Category: Physiology, Medical Sciences

Metabolic Regulation of Female Puberty via Hypothalamic AMPK-Kisspeptin Signaling

Juan Roa[1,2,3,4]*, Alexia Barroso[1,2,3,4]¶, Francisco Ruiz-Pino[1,2,3,4]¶, Maria Jesus Vázquez[1,2,3,4], Patricia Seoane-Collazo[4,5], Noelia Martínez-Sanchez[4,5], David García-Galiano[1,2], Tuncay Ilhan[1,2], Rafael Pineda[1,2,3,4], Silvia León[1,2], Maria Manfredi-Lozano[1,2], Violeta Heras[1,2], Matti Poutanen[6], Juan M Castellano[1,2,3,4], Francisco Gaytan[1,2,3,4], Carlos Diéguez[4,5], Leonor Pinilla[1,2,3,4], Miguel López[4,5], Manuel Tena-Sempere[1,2,3,4,6]*

[1]Instituto Maimónides de Investigación Biomédica de Cordoba (IMIBIC); [2]Department of Cell Biology, Physiology and Immunology, University of Cordoba; [3]Hospital Universitario Reina Sofia; and [4]CIBER Fisiopatología de la Obesidad y Nutrición, Instituto de Salud Carlos III, 14004 Cordoba, Spain; [5]NeurObesity Group, Department of Physiology, Faculty of Medicine and CIMUS, University of Santiago de Compostela-Instituto de Investigación Sanitaria, 15782 Santiago de Compostela, Spain; and [6]Institute of Biomedicine, Department of Physiology, University of Turku, Turku, Finland

*Co-corresponding authors

¶Equally contributed and should be considered joint second authors

Short Title: Metabolic regulation of puberty by AMPK via Kiss1

Key Words: AMPK, Kiss1, kisspeptins, energy balance, undernutrition, puberty

Corresponding authors: Juan Roa (roarivas@gmail.com) and
Manuel Tena-Sempere (fi1tesem@uco.es)
Department of Cell Biology, Physiology & Immunology
Faculty of Medicine, University of Córdoba
Avda. Menéndez Pidal s/n. 14004 Córdoba, SPAIN

Legend to Supplemental Figures

SI Appendix Fig. S1: *Central infusion of AICAR activates hypothalamic AMPK*.

Western blots are shown on the hypothalamic content of pAMPK (**A**, **B**), α1- and α2-AMPK subunits, and the down-stream factor, ACC and p-ACC (**C**), in pubertal female rats after chronic icv infusion of the pharmacological activator of AMPK, AICAR. Pair-aged females chronically treated with vehicle served as controls. Quantitative analyses of the ratios between phosphor- and total content of each factor are also presented as histograms. Since pAMPK ratios were calculated for both subunits, note that the same representative pAMPK panel is presented in **A** and **B** panel. **P*<0.05; ** *P*<0.01 *vs*. corresponding control groups (Student t-tests; n=5 independent animals per group).

SI Appendix Fig. S2: *Central infusion of AICAR does not increase pAMPK levels in the cortex or hippocampus*

Western blots are shown of the content of pAMPK in the cortex (**A**) and hippocampus (**B**) of pubertal female rats after chronic icv infusion of the pharmacological activator of AMPK, AICAR. Pair-aged females treated with vehicle served as controls. Quantitative analyses of the expression levels of pAMPK, normalized to β-actin, are also presented as histograms. No significant differences were detected between groups (Student t-tests; n=5 independent animals per group). In addition, in the lower panel (**C**), representative images of immunohistochemistry of pAMPK in the different brain areas analyzed (hippocampus: HC; cortex: CX; hypothalamus: HTAL), as well as a cartoon depicting these areas are shown. In addition, quantitative analysis of the percentage of pAMPK staining per each brain area, evaluated in pubertal female rats in control conditions, is presented. Histograms with different superscript letters were statistically different (*P*<0.05; ANOVA followed by Student-Newman-Keuls multiple range test).

SI Appendix Fig. S3: *Virogenetic overexpression of AMPK in the VMH does not delay puberty onset*

In panel **A**, a schematic representation of the bilateral stereotaxic injection of viruses inducing over-expression of a constitutively active form of AMPK (AMPK-CA) in the ventromedial hypothalamus (VMH), is shown. Representative images, at two different magnifications, of bilateral targeting of the VMH, as denoted by fluorescein labeling, are also presented in panels **B** and **C**, while efficiency of adenoviral-mediated infection of VMH neurons by stereotaxic delivery is documented by GFP labeling, as shown in panel **D**. In addition, the impact of such AMPK-CA over-expression on BW (**E**), the

percentage of vaginal opening (VO; **F**) and serum LH levels (as marker of activation of the reproductive axis; **G**) is depicted. Animals injected with viral vectors over-expressing only the marker, GFP, were used as controls. Due to co-administration of fluorescein isothiocyanate in both GFP and AMPK-CA treated animals, the injection site was evaluated post-mortem, and animals with evidence for off-target injections were not considered from further analyses. Final group sizes (i.e., animals with proper viral injections) were: Control-GFP =9; AMPK-CA=11 animals/group. **P*<0.05 *vs*. corresponding control-GFP group (Student t-tests).

SI Appendix Fig. S4: *Orthogonal and 3D analyses of pAMPK co-expression in ARC Kiss1 neurons*

In panel **A**, the orthogonal view of the confocal image presented in Figure 3, demonstrating co-localization of pAMPK (red) and DAPI (blue) in a Kiss1 neuron (green), is shown. XZ and YZ views demonstrate that nuclear pAMPK immunoreactivity (red) is contained within Kiss1 neurons (green). Co-localization of pAMPK with DAPI results in magenta. In panel **B**, a representative 3D reconstruction of two Kiss1 neurons (green), co-expressing pAMPK (red), is presented. An enlarged view of the white square area and internal view of the exampled neuron, by using the clipping plane tool in Imaris, are presented in the middle and right pictures, respectively.

SI Appendix Fig. S5: *Genotyping and validation of Kiss1-specific AMPK null (KAMKO) mice*

In panel **A**, representative genotyping results on the presence of AMPKα1 loxP and the Kiss1-driven Cre alleles are shown. For AMPK$\alpha1^{loxP}$, the 334-bp amplicon denotes wild type (WT) and the 450-bp fragment the floxed allele; representative examples of one WT and one heterozygous mouse (the latter harboring one loxP-flanked allele) are provided in lanes 1 and 2, respectively. For Kiss1-Cre, the 337-bp amplicon represents the wild type allele and the 250-bp amplicon the Cre allele; representative examples are shown in lanes (a) and (b), respectively. In addition, in panel **B**, PCR results showing successful recombination of the AMPKα1 loxP allele in hypothalamic areas, POA and ARC (that hold Kiss1 neurons), but not in the cortex are shown in two independent KO mice. In contrast, control mice did not present evidence of recombination in any tissue tested. Effective recombination is denoted by the appearance of a 530-bp amplicon in the PCR assay. Finally, in panel **C**, representative images at different magnifications of double immunohistochemical assays, detecting GFP-tagged Cre and kisspeptin, are shown for the two main population of Kiss1 neurons, located in the AVPV (top images) and ARC (bottom images). GFP staining (black) presented a nuclear localization, surrounded by kisspeptin immunoreactivity (brown).

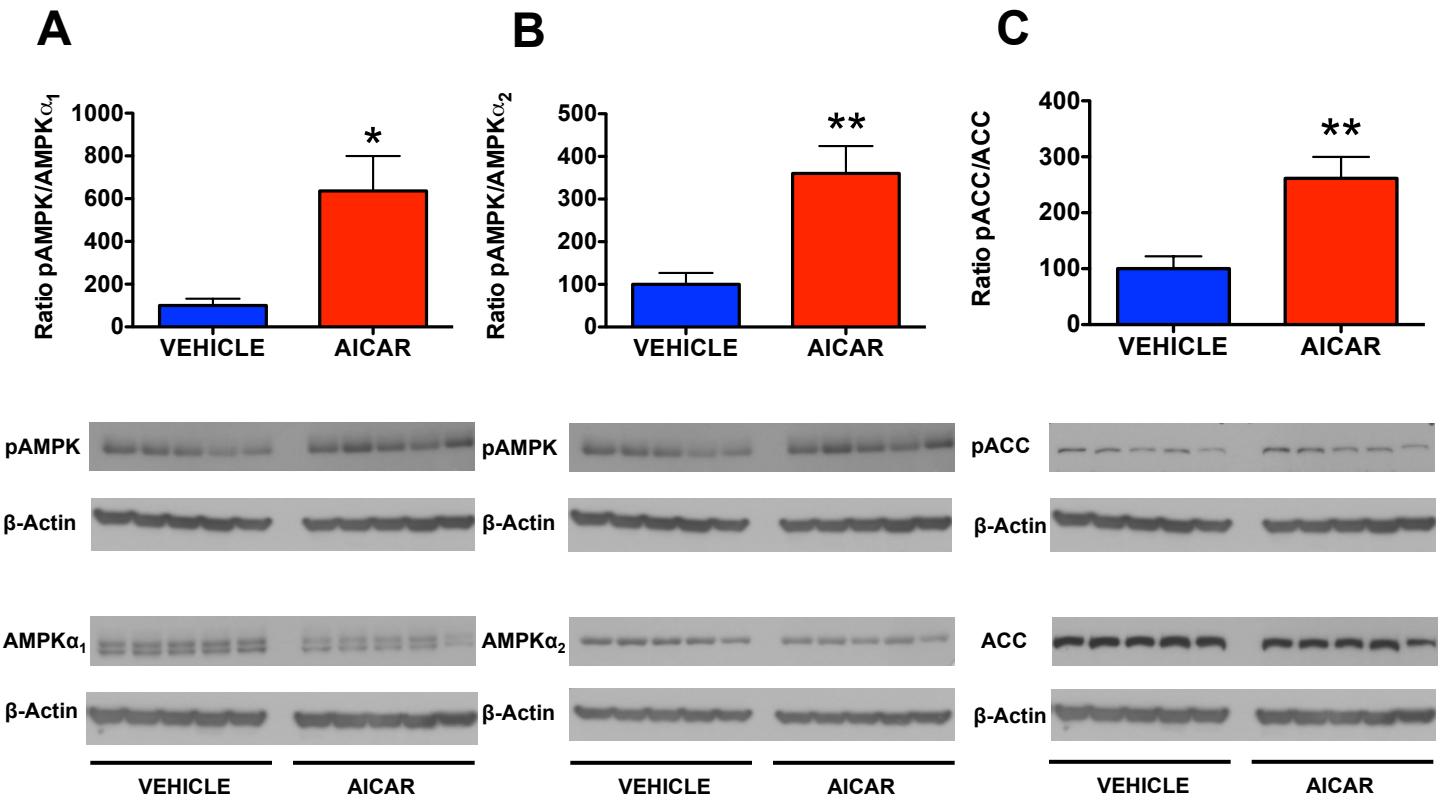

SI Appendix Fig. S1

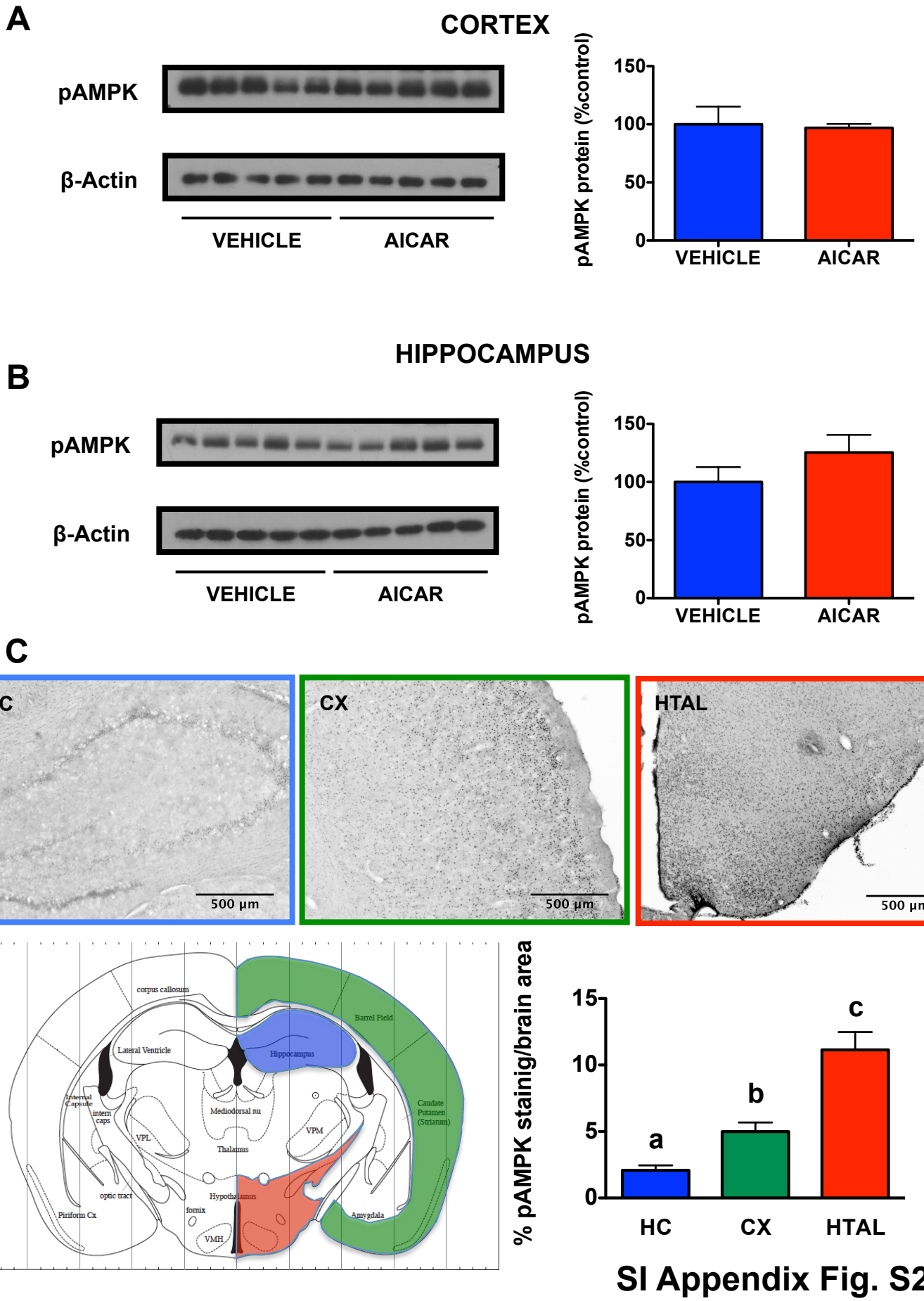

SI Appendix Fig. S2

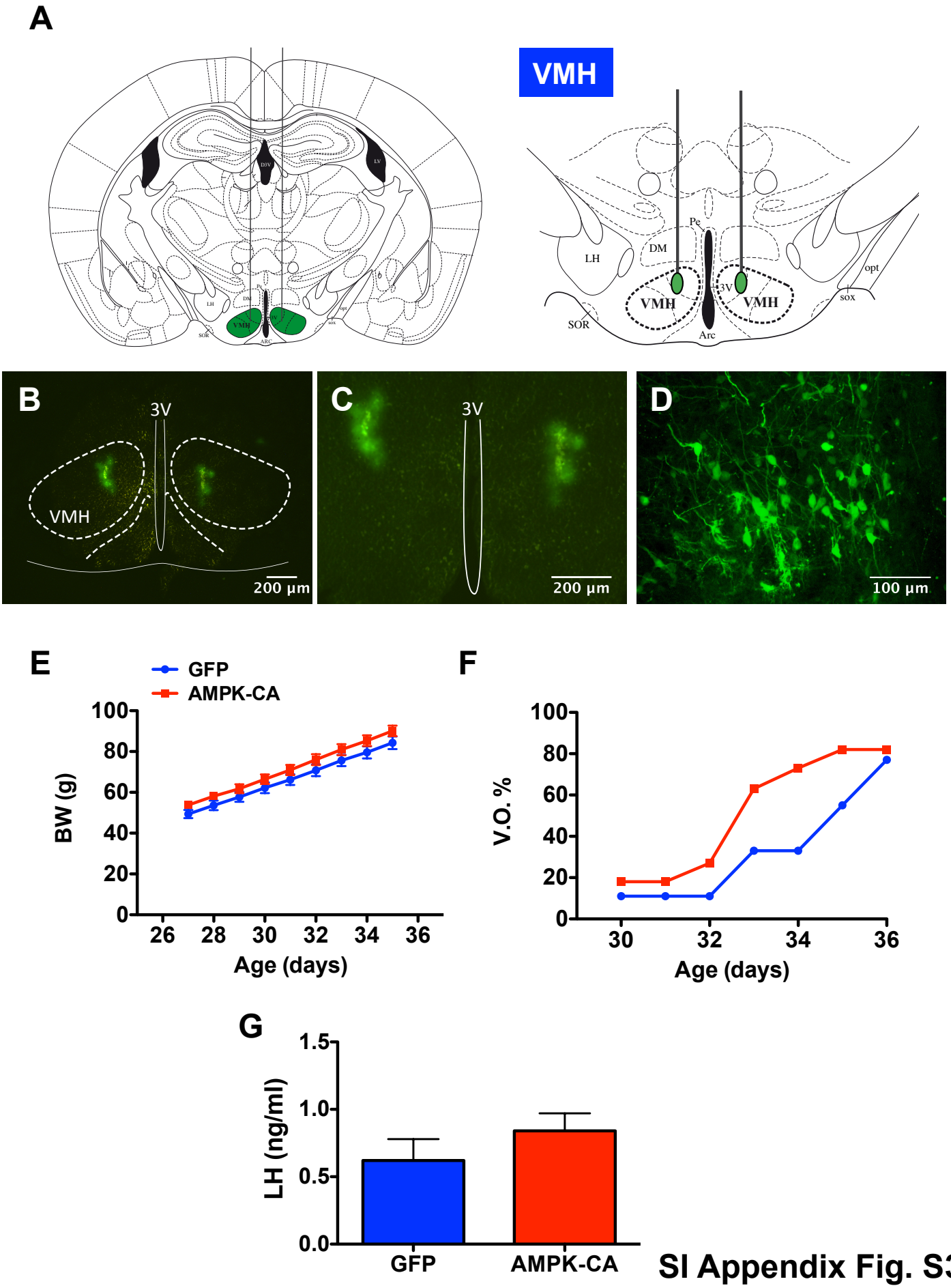

SI Appendix Fig. S3

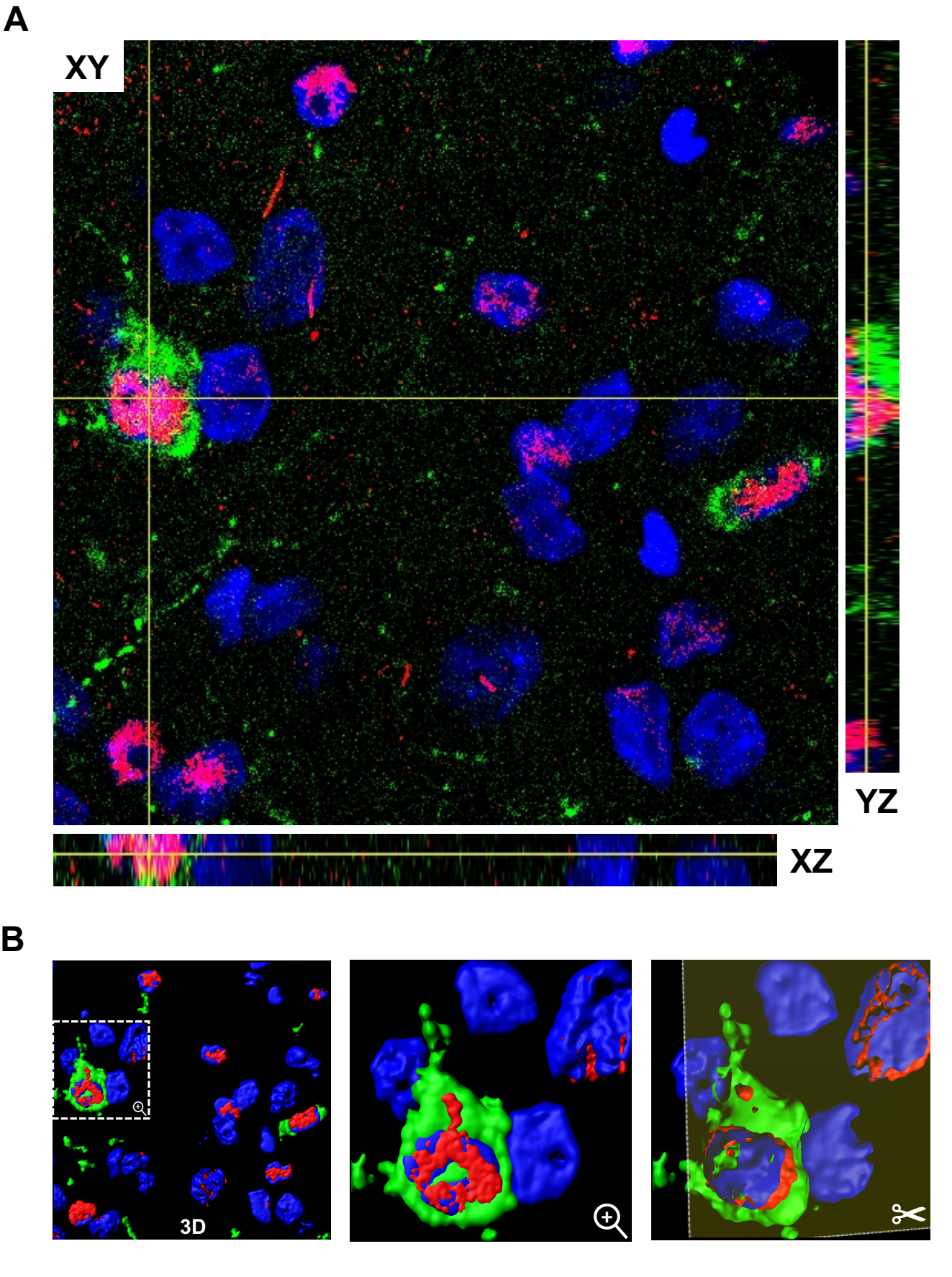

SI Appendix Fig. S4

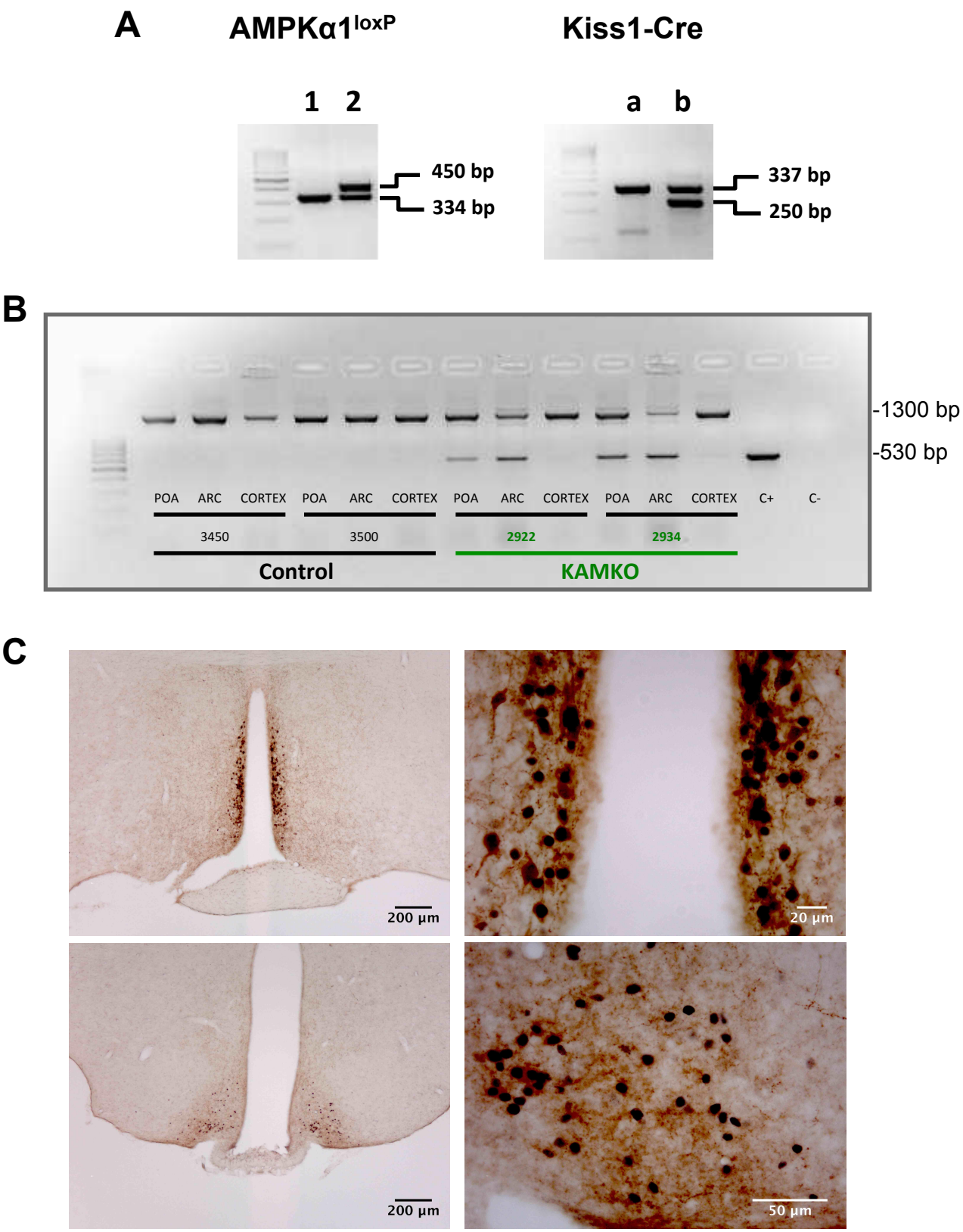

SI Appendix Fig. S5